Energetics of Two-Step Binding of a Chromophoric Reaction Product, *trans*-3-Indoleacryloyl-CoA, to Medium-Chain Acyl-Coenzyme-A Dehydrogenase†

Ling Qin and D. K. Srivastava*

Biochemistry Department, North Dakota State University, Fargo, North Dakota 58105

Received August 19, 1997; Revised Manuscript Received January 6, 1998

ABSTRACT: We previously demonstrated that the UV/visible spectrum of a chromophoric ligand, *trans*-3-indoleacryloyl-coenzyme-A (IACoA), is red-shifted (due to polarization of its carbonyl group) upon binding to pig kidney medium-chain acyl-CoA dehydrogenase (MCAD). The transient kinetic data revealed that the overall binding occurred in two steps. The first (fast) step involved the formation of an MCAD−IACoA collision complex in which the electronic structure of IACoA remained unchanged (the "colorless" complex), followed by a slow isomerization step with a concomitant red-shift in the IACoA spectrum (the "colored" complex) [Johnson, J. K., Wang, Z. X., and Srivastava, D. K. (1992) *Biochemistry 31,* 10564−10575]. To ascertain the energetics of the above two-step process, we investigated the temperature dependence of the spectral changes, binding constant of the MCAD−IACoA complex, and the rate constants for the conversion between the colorless and colored complexes. The data revealed that as the temperature of the incubation mixture of MCAD and IACoA ([IACoA] ≫ [MCAD] > K_d) increases from 12 to 35 °C, the resultant spectral peak of the MCAD−IACoA complex (λ_{max} = 417 nm) decreases. However, in this temperature range, the equilibrium constant for the second (isomerization) step remains unaffected. Isothermal titration calorimetric studies for the binding of IACoA to MCAD reveal that the overall binding energy at 25 °C ($\Delta G°$ = −7.4 kcal/mol) is contributed almost equally by the enthalpic ($\Delta H°$ = −3.7 kcal/mol) and entropic ($T\Delta S°$ = 3.7 kcal/mol) changes. As the temperature increases, both $\Delta H°$ and $T\Delta S°$ decrease proportionately, resulting in a strong enthalpy−entropy compensation effect. The temperature dependence of $\Delta H°$ yields a $\Delta C_p°$ value of −0.24 kcal/mol. The data presented herein throw light on the energetic consequences for the binding of IACoA to MCAD, the apparent similarity between the van't Hoff and calorimetric enthalpies, enthalpic and entropic contributions during the polarization of the carbonyl group of IACoA, and the overall structural-functional features of the enzyme−ligand complex as well as the enzyme catalysis.

In pursuit of delineating the kinetic mechanism of medium-chain acyl-coenzyme-A (acyl-CoA) dehydrogenase (MCAD),[1] we introduced 3-indolepropionyl-CoA (IPCoA) as a chromogenic substrate (*1, 2*). As noted with other acyl-CoA substrates, the enzyme catalysis was found to proceed via two discrete steps (for recent reviews, see refs *3*−*5*; eq 1).

$$\text{E}-\text{FAD} + \text{acyl-CoA} \rightleftharpoons \text{E}-\text{FADH}_2-\text{enoyl-CoA} \quad (1A)$$

$$\text{E}-\text{FADH}_2-\text{enoyl-CoA} + \text{ETF}-\text{FAD} \rightleftharpoons \text{E}-\text{FAD}-\text{enoyl-CoA} + \text{ETF}-\text{FADH}_2 \quad (1B)$$

The first step, referred to as the "reductive half-reaction" (eq 1A) involves the reduction of the enzyme-bound FAD to $FADH_2$ with concomitant oxidation of IPCoA to *trans*-3-indoleacryloyl-CoA (IACoA). Due to a marked kinetic and thermodynamic stability of the E−$FADH_2$−IACoA complex (against oxidation by the buffer-dissolved oxygen), the latter predominates as a major enzyme species in the oxygenated buffer medium. The repetitive turnover of the enzyme is maintained via oxidation of the E−$FADH_2$−IACoA complex by "organic" electron acceptors, such as electron-transferring flavoprotein (ETF) or ferrocenium hexafluorophosphate ($FcPF_6$) during the second half-reaction, referred to as the "oxidative half-reaction" (eq 1B) of the enzyme.

One of the major advantages of utilizing IPCoA as a chromogenic substrate (vis à vis aliphatic acyl-CoAs) was that the reaction product IACoA showed a strong absorption band in the near visible region (λ_{max} = 367 nm, $\epsilon_{367} = 2.65 \times 10^4$ M^{-1} cm^{-1}), and thus the enzyme catalysis could be easily monitored without recourse to the spectral signals of the "colored" electron acceptors, such as $FcPF_6$, DCPIP, etc. (*1, 6)*. Such a feature of IACoA allowed us to investigate the structural-functional aspects of the enzyme catalysis and

† This work was supported by grants from the National Science Foundation (MCB-9507292) and the American Heart Association, National Center (AHA-96008200).

* To whom correspondence should be addressed.

[1] Abbreviations: MCAD, medium-chain acyl-CoA dehydrogenase; FAD, flavin adenine dinucleotide; IPCoA, 3-indolepropionyl coenzyme-A; IACoA, *trans*-3-indoleacryloyl coenzyme-A, $FcPF_6$, ferrocenium hexafluorophosphate; ETF, electron-transferring flavoprotein; $\Delta H°$, standard enthalpy change, $\Delta S°$, standard entropy change; $\Delta G°$, standard free energy change; $\Delta C_p°$, heat capacity change; ΔS_{rt}, rotational and translational entropy change, ΔS_v, vibrational entropy change, ΔS_{HE}, entropy change due to hydrophobic interaction; ΔS_{conf}, conformational entropy change; K_a, association constant; K_c, dissociation constant of the collision complex; EDTA, ethylenediaminetetraacetic acid.

S0006-2960(97)02058-8 CCC: $15.00
Published on Web 02/18/1998

the enzyme−ligand interactions under diverse experimental conditions (*7*−*9*, *10*, *11*).

We previously reported that the binding of IACoA to E−FAD results in a red-shift in the electronic spectrum of IACoA (*1*). Such a red-shift has been found with a number of chromophoric acyl-CoA analogues such as furylacryloyl-CoA (*10*), cinnamoyl-CoA (*12*), 4-(dimethylamino)cinnamoyl-CoA (*10*), 4-aminobenzoyl-CoA (*13*), and 4-thia-2-octenoyl-CoA (*14*), upon binding to the enzyme site. With precedents of the enzymological literature dealing with the interaction of chromophoric ligands with their cognate enzymes (*15*−*17*), the red-shifted spectra of the above CoA derivatives have been attributed to polarization of their carbonyl groups (*1, 10*). This conclusion is supported by the X-ray crystallographic structure of the enzyme−octenoyl-CoA complex, which shows a strong hydrogen bonding between the carbonyl oxygen of octenoyl-CoA and the 2′-ribityl hydroxyl group of FAD as well as with the main chain amide nitrogen of Glu-376 (*18*). The fact that the 2′-deoxy derivative of FAD results almost in a complete loss of the enzyme activity, utilizing octanoyl-CoA as a substrate, attests to the functional role of the 2′-ribityl hydroxyl group of FAD during the enzyme catalysis (*19*).

By employing the transient kinetic techniques, we probed the sequence of events leading to the polarization of the carbonyl group of IACoA upon interaction with the oxidized enzyme site (*1*, *8*, *9*). Under pseudo-first-order conditions ([IACoA] ≫ [MCAD]), the rate of increase in absorption at 417 nm (the absorption maximum of the MCAD−IACoA complex) conformed to a single-exponential rate law, and the observed rate constant exhibited a hyperbolic dependence on IACoA concentration, suggesting that the binding of IACoA to MCAD occurred following the formation of the MCAD−IACoA collision complex (*1*). The latter species underwent a slow isomerization reaction (presumably via the protein conformational changes) with polarization of the carbonyl group of IACoA. Since no absorption changes were detected at 417 nm within the dead time of our stopped flow, we proposed that the polarization of the carbonyl group of IACoA occurred during isomerization of the MCAD−IACoA collision complex (*1*, *8*, *9*). Hence, the collision and the isomerized complexes are referred to as the "colorless" and "colored" complexes, respectively (eq 2). In eq 2, K_c

$$\text{MCAD} + \text{IACoA} \underset{K_c}{\rightleftharpoons} \underset{\text{"colorless" collision complex}}{\text{MCAD−IACoA}} \underset{k_{-2}}{\overset{k_2}{\rightleftharpoons}} \underset{\text{"colored" isomerized complex}}{\text{MCAD−IACoA*}} \quad (2)$$

represents the dissociation constant of the MCAD−IACoA collision complex, and k_2 and k_{-2} represent the forward and reverse rate constants for the conversion of MCAD−IACoA collision complex to MCAD−IACoA* isomerized complex, respectively.

We became interested in the nature and magnitudes of the physical forces responsible for promoting the individual (i.e., ligand binding and isomerization) steps upon interaction of IACoA with the enzyme. We recently investigated the binding of octenoyl-CoA (the reaction product of the physiological substrate octanoyl-CoA) to pig kidney MCAD via isothermal titration microcalorimetry (*20*). These studies revealed that at all temperatures >25 °C, the binding of octenoyl-CoA to MCAD was dominated by favorable enthalpic changes with a large negative (−0.37 (kcal/mol)/K) value of ΔC_p°. The latter was suggestive of a strong hydrophobic interaction between octenoyl-CoA and protein (*20*). However, due to the lack of pronounced spectral signal with the enzyme−octenoyl-CoA complex as well as due to the inherent complexity of the overall binding steps (*21, 22*), we could not discern the energetics of the individual microscopic steps of the overall binding pathway. Since such limitations were not evident with IACoA (being a chromophoric reaction product of the enzyme), we hoped to ascertain the thermodynamic contributions of the individual steps by employing both spectrophotometric and microcalorimetric methods.

MATERIALS AND METHODS

Materials. Coenzyme A (sodium salt) and acetoacetyl CoA (sodium salt) were purchased from Sigma. 3-Indolepropionic acid and *trans*-3-indoleacrylic acid, were purchased from Aldrich. Other reagents were of analytical grade.

Methods. All experiments were performed in 50 mM potassium phosphate buffer (pH 7.6) containing 0.3 mM EDTA and 100 mM KCl, unless stated otherwise. Steady-state kinetic experiments and spectral acquisitions were performed either on a Perkin-Elmer Lambda 3B or on Beckman 7400 spectrophotometer.

The CoA derivatives, indolepropionyl-CoA (IPCoA) and indoleacryloyl-CoA (IACoA), were synthesized and purified as described by Johnson et al. (*1*). The extinction coefficients of IPCoA and IACoA were taken to be 18.2 mM^{-1} cm^{-1} (at 259 nm) and 26.5 $mM^{-1}cm^{-1}$ (at 367 nm), respectively (*1*).

Pig kidney MCAD was purified and routinely assayed in the 50 mM potassium phosphate buffer (pH 7.6) containing 0.3 mM EDTA, utilizing 120 μM IPCoA and 100 FM ferrocenium hexafluorophosphate ($FcPF_6$) as an electron acceptor as described by Johnson et al. (*1*). The enzyme concentration was determined by using an extinction coefficient of 15.4 mM^{-1} cm^{-1} at 446 nm (*23*).

The steady-state kinetic experiments for the IPCoA-dependent reaction were performed by monitoring the absorption changes at 367 nm on a Lambda 3B Perkin-Elmer spectrophotometer. The temperature of the reaction mixture was maintained by circulating water from a temperature-controlled bath to the thermostated cuvette holder. The reaction mixture was continuously stirred with the aid of a magnetic stirrer installed at the bottom of the cuvette holder.

Transient Kinetic Experiments. Transient kinetic experiments were performed on an Applied Photophysics SX-17 MV sequential mixing stopped-flow system (optical path length = 10 mm, dead time = 1.3−1.5 ms) in a single mixing mode as described previously (*8*, *9*, *21*, *22*, *24*). The stopped-flow kinetic traces were analyzed by the data analysis package provided by Applied Photophysics.

Spectrophotometric Titration of MCAD with IACoA. The binding constant of the MCAD−IACoA complex was determined by spectrophotometric titration (at 417 nm) of a fixed concentration of MCAD (approximately 8 μM) and increasing concentrations of IACoA. The absorbance of IACoA and MCAD at 417 nm were subtracted from the absorbance of their mixture at the same wavelength following

a dilution correction. The increase in absorbance at 417 nm as a function of total concentration of IACoA was analyzed according to eq 3. In eq 3, K_d, n, E_t, I_t, and $\Delta\epsilon$, refer to the

$$\Delta A_{417} = \Delta\epsilon\left\{\frac{(nE_t + I_t + K_d) - \sqrt{(nE_t + I_t + K_d)^2 - 4nE_tI_t}}{2}\right\} \quad (3)$$

dissociation constant of the enzyme−IACoA complex, stoichiometry of the enzyme−IACoA complex, total enzyme concentration, total IACoA concentration, and the difference in molar extinction coefficients of the complex minus its individual components, respectively. The association constant (K_a) of the enzyme-IACoA complex was taken as the reciprocal of the dissociation constant (K_d).

The enzyme-IACoA titration data were fitted by eq 3 using the nonlinear regression analysis method (based on the Levenberg−Marquardt algorithm) by Grafit (Erithacus, Software Ltd., U.K.) software. The curve fitting was accomplished in two stages. The first step involved fixing the total concentration of the enzyme (E_t) and stoichiometry of the enzyme-IACoA complex (n) to be 1.0. The magnitudes of $\Delta\epsilon$ and K_d derived from the above analysis were used as initial estimates for the final curve fitting. During the latter stage, except for E_t (which was fixed), other parameters of eq 3 were allowed to vary, and the iterations were continued until the convergence (minimum χ^2 value) was achieved. Such analysis yielded the magnitudes of $\Delta\epsilon$, K_d, and n. The standard deviation was obtained from the best fit of the single titration data.

Isothermal Titration Microcalorimetry. All calorimetric experiments were conducted on an MCS isothermal titration calorimeter (ITC) from Microcal, Inc. (Northampton, MA). A complete description of its predecessor instrument, OMEGA-ITC, experimental strategies, and data analysis are given by Wiseman et al. (*25*). The calorimeter was calibrated by known heat pulses as described in the MCS-ITC manual. During titration, the reference cell was filled with 0.03% azide solution in water. Prior to the titration experiment, both enzyme and IACoA were thoroughly degassed under vacuum. The sample cell was filled either with 1.8 mL (effective volume = 1.36 mL) of buffer (for control) or with appropriately diluted enzyme. The contents of the sample cell was titrated with 40 aliquots of IACoA. During the titration, the reaction mixture was continuously stirred at 400 rpm. The enzyme concentration was adjusted by 2% (as recommended by the manufacturer) to include a dilution effect of the enzyme solution, which occurs following a buffer rinse.

All calorimetric titration data were presented after subtracting the corresponding background. The background titration profiles, under identical experimental conditions, were obtained by injecting IACoA into appropriate buffer solutions. The raw data were presented as the amount of heat produced per second following each injection of ligand into the enzyme solution (minus the blank) as a function of time. The amount of heat produced per injection was calculated by integration of the area under individual peaks by the Origin software, provided with the instrument. Final data are presented as the amount of heat produced per injection versus the molar ratio of IACoA to MCAD. The data were analyzed by the Origin software as described by Wiseman et al. (*25*). All parameters (viz., n, K_a, and $\Delta H°$) were allowed to vary during the curve fitting. Unless noted otherwise, the standard errors were derived from the best fit of the single titration data.

The data analysis produced three parameters, viz., stoichiometry (n), association constant (K_a), and the standard enthalpy changes ($\Delta H°$), for the binding of IACoA to MCAD. The standard free energy change ($\Delta G°$) for the binding was calculated according to the relationship, $\Delta G° = -RT \ln K_a$. Given the magnitudes of $\Delta G°$ and $\Delta H°$, the standard entropy changes ($\Delta S°$) for the binding process were calculated according to the standard thermodynamic equation, $\Delta G° = \Delta H° - T\Delta S°$.

RESULTS

Johnson et al. (*1*) described that the absorption spectrum of pig kidney medium-chain acyl-CoA dehydrogenase (MCAD) is drastically altered in the presence of indoleacryloyl-CoA (IACoA) as a chromophoric reaction product. The difference spectrum (i.e., the spectrum of the mixture minus the individual components) is marked by major positive and negative absorption bands at 417 and 355 nm, respectively, and a minor positive band at 486 nm. With precedents of the spectral features of several different chromophoric enoyl-CoA analogues (see Introduction), the spectral band at 417 nm has been ascribed to originate (at least in part) due to polarization of the carbonyl group of IACoA.

Effect of Temperature on the Magnitude of the 417 nm Absorption Band. We investigated the effect of temperature on the magnitude of the spectral band at 417 nm. During this experiment, the temperature of the incubation mixture containing 10.5 μM MCAD and 92 μM IACoA was increased from 12 to 35 °C in the spectrophotometric cell (equipped with a Peltier temperature controller), and following the attainment of the desired temperature, the spectrum of the mixture was recorded. As a control, the spectra of MCAD and IACoA were individually recorded at the corresponding temperatures. Figure 1 shows the temperature dependence of the spectral changes (i.e., the spectrum of the mixture minus its individual components). Since, during these experiments, we employed a high concentration of IACoA (so as to saturate the enzyme at all temperatures), the background absorption of the reaction mixture was considerably high, particularly at lower wavelength regions. Hence, the difference spectra have been presented only in the 396 and 510 nm region. The inset of Figure 1 shows a temperature dependence of ΔA_{417}. Note a decrease in the magnitude of ΔA_{417} with an increase in the incubation temperature. A similar trend is also apparent at 486 nm, although the magnitude of the spectral changes is not as pronounced (due to a lower extinction coefficient) as that at 417 nm. Assuming that the spectral band at 417 nm is primarily due to polarization of the carbonyl group of IACoA, the data of Figure 1 suggest that the extent of polarization decreases with an increase in temperature.

Binding of IACoA to E−FAD. (A) Spectrophotometric Studies. By utilizing the signal for interaction of IACoA to MCAD at 417 nm, we could determine the binding constants

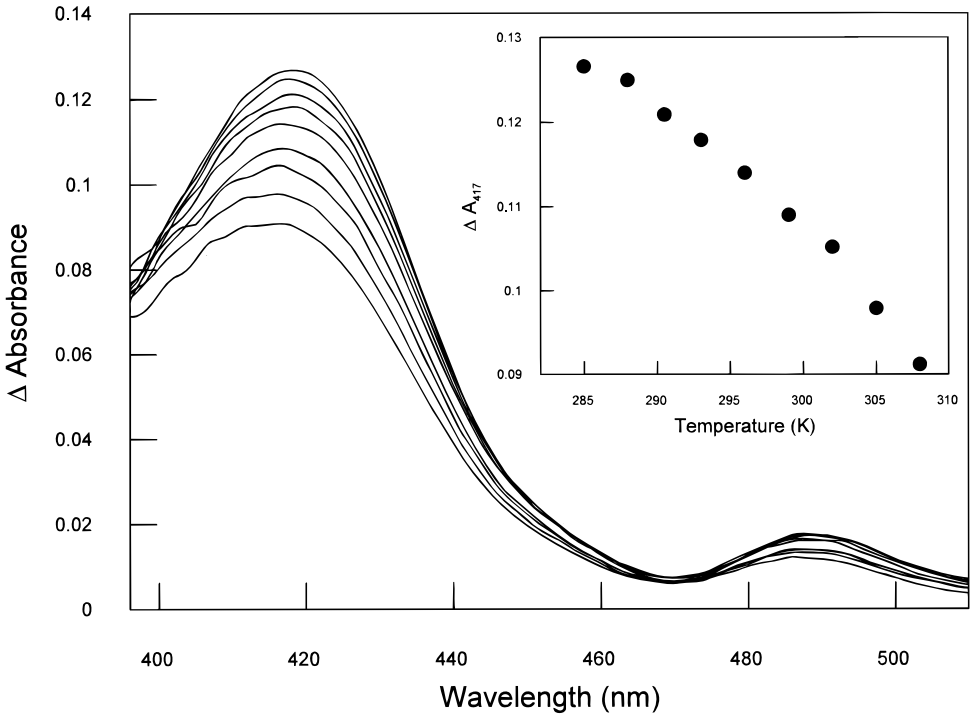

FIGURE 1: Effect of temperature on the spectral properties of the enzyme−IACoA complex. These spectra were generated following a rapid change of temperature of the reaction mixture containing 10.5 μM MCAD−FAD and 92 μM IACoA. The contributions of MCAD−FAD and IACoA at corresponding temperatures were subtracted from the spectra of the mixture. The inset shows the absorption changes at 417 nm as a function of temperature.

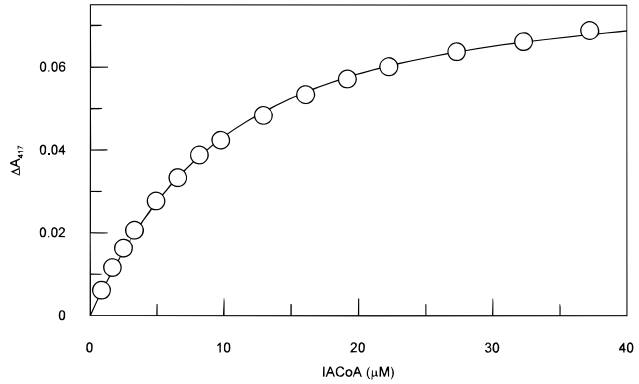

FIGURE 2: Representative binding isotherm for the interaction of IACoA to MCAD at 25 °C. [MCAD] = 8.0 μM. The solid smooth line is the best fit of the data by eq 3, with an association constant of (1.61 ± 0.05) × 10^5 M^{-1} and stoichiometry of 0.65 ± 0.02 mol of IACoA/mol of MCAD subunit.

of the above species as a function of temperature. A typical binding isotherm for the association of IACoA to MCAD at 25 °C is shown in Figure 2. During this experiment, 8.0 μM MCAD was titrated with increasing concentrations of IACoA, and the net increase in absorption at 417 nm (after dilution correction) is plotted as a function of total concentration of IACoA. Since the concentration of IACoA was comparable to the concentration of MCAD, the dissociation constant of the MCAD−IACoA complex (K_d) and the stoichiometry of the MCAD−IACoA complex were determined by analyzing the data by eq 3. The solid smooth line is the best fit of the data for a dissociation constant (K_d) of 6.2 ± 0.2 μM and stoichiometry of 0.65 ± 0.02 (mole of IACoA/MCAD subunit), respectively. The association constant (K_a) derived from the above data ($K_a = 1/K_d$) was (1.61 ± 0.05) × 10^5 M^{-1}.

Table 1: Effect of Temperature on Association Constant (K_a) of the MCAD−IACoA Complex[a]

temp (K)	n	$10^{-5}K_a$ (M^{-1})
286	0.69 ± 0.012	1.91 ± 0.05
288	0.68 ± 0.013	1.94 ± 0.06
293	0.56 ± 0.016	1.76 ± 0.07
298	0.65 ± 0.016	1.61 ± 0.05
301	0.76 ± 0.038	1.61 ± 0.11
306	0.79 ± 0.018	1.39 ± 0.04
308	0.72 ± 0.020	1.18 ± 0.04

[a] Determined by the spectrophotometric titration method.

To ascertain the effect of temperature on the association constant of the MCAD−IACoA complex, we performed the above titration experiments at different temperatures. The association constants and stoichiometries derived from such titration data are summarized in Table 1. Note that as the temperature of the incubation mixture increases from 13 to 35 °C, the association constant decreases from 1.91 × 10^5 to 1.18 × 10^5 M^{-1}.

Figure 3 shows the van't Hoff plot for the binding of IACoA to MCAD. The solid smooth line is the best fit of the data according to the linear van't Hoff equation in the following format (eq 4), where K_a, A, ΔH_{vH}, and R are the

$$\ln K_a = \ln A - \frac{\Delta H_{vH}}{RT} \quad (4)$$

association constant of the enzyme-IACoA complex, the entropic factor, the van't Hoff enthalpy, and the universal gas constant, respectively.

The van't Hoff enthalpy (ΔH_{vH}) calculated from the linear dependence of ln K_a on $1/T$ yields a value of −3.43 kcal/mol. However, the correspondence between the data and

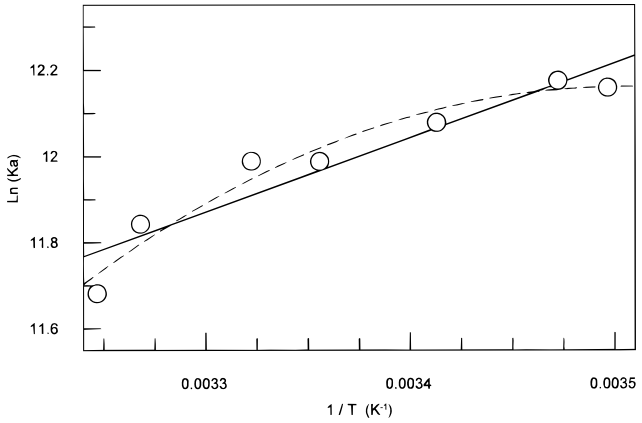

FIGURE 3: van't Hoff plot for the binding of IACoA to MCAD. The association constant for the MCAD−IACoA complex as a function of temperature was determined as described in Figure 2. The solid and broken smooth lines are the best fit of the data according to linear (eq 4) and integrated (eq 5) van't Hoff equations. The magnitudes of ln A and ΔH_{vH} derived from the best fit of the data according to eq 4 were 6.18 and −3.43 kcal/mol, respectively, and those of T_r, ΔH_r, ΔC_p, and K_r derived from the best fit of the data according to eq 5 were 295.5 K, −3.07 kcal/mol, −0.303 (kcal/mol)/K, and 1.75×10^5 M^{-1}, respectively.

the fitted line is not so great ($r = 0.946$). It should be noted that the above analysis relies on the fact that the heat capacity changes ($\Delta C_p°$) during the enzyme-IACoA interaction is equal to zero. This is clearly not the case since $\Delta H°$ for the binding of IACoA to the enzyme, measured via the isothermal microcalorimetric method, shows a strong temperature dependence (see below). In light of this consideration, we analyzed the data of Figure 3 by an integrated form of the van't Hoff equation, which incorporates the $\Delta C_p°$ term (*26*; eq 5), where T_r is an arbitrarily chosen reference temperature

$$\ln K_a = \ln K_r + \frac{\Delta H_r - T_r \Delta C_p}{R}\left(\frac{1}{T_r} - \frac{1}{T}\right) + \frac{\Delta C_p}{R} \ln \frac{T}{T_r} \quad (5)$$

and K_r and ΔH_r are the temporarily assigned association constant and van't Hoff enthalpy, respectively, at that temperature. ΔC_p is the heat capacity change. The broken line of Figure 3 represents the best fit of the data according to eq 5, for the van't Hoff enthalpy of −3.07 kcal/mol at 295.5 K and ΔC_p value of −0.303 (kcal/mol)/K. Although the fitted line is somewhat better than that obtained via linear van't Hoff analysis (eq 4), it is, by no means, the best. We believe the lack of correspondence between experimental and theoretical lines is due to small errors in determining the temperature dependence of the association constants of the enzyme-IACoA complex.

(B) Microcalorimetric Studies. We investigated the interaction of IACoA to MCAD via isothermal titration microcalorimetry. Figure 4 shows the titration of 9.8 μM MCAD by increasing aliquots (first aliquot = 1 μL, and subsequent 39 aliquots = 4 μL each) of IACoA (stock concentration = 0.59 mM) at 25 °C. The top panel shows the raw calorimetric data, denoting the amount of heat produced (negative exothermic peaks) following each injection of IACoA. The area under each peak represents the amount of heat produced upon binding of IACoA to MCAD. Note that as the titration progresses, the area under the peaks progressively becomes smaller due to an increased occupancy of the enzyme by IACoA. The bottom panel of Figure 4

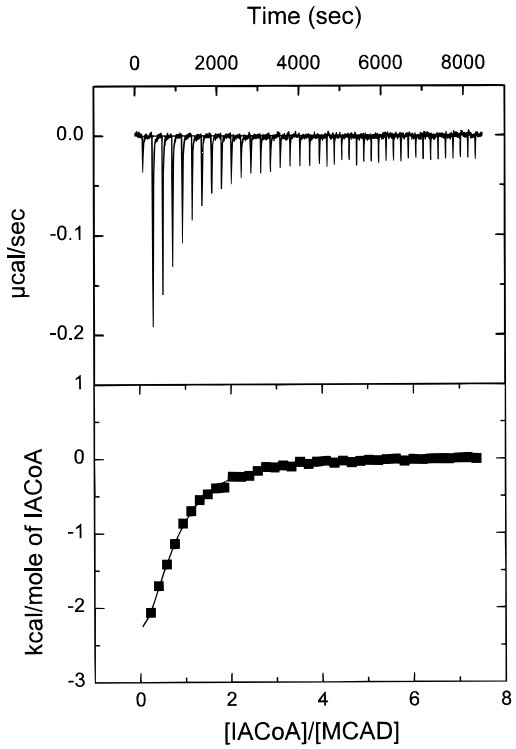

FIGURE 4: Microcalorimetric titration of MCAD by IACoA at 25 °C. Panel A (top) shows the raw data, generated by titration of 1.8 mL of 9.8 μM MCAD by forty (first injection = 1 μL, subsequent 39 injections = 4 μL each) injections of 590 μM IACoA. The area under each peak was integrated and plotted against the molar ratio of IACoA to MCAD in panel B (bottom). The solid smooth line is the best fit of the data for the stoichiometry of the MCAD−IACoA complex (moles of bound IACoA per mole of MCAD subunit) of 0.65, association constant (K_a) of 2.6×10^5 M^{-1}, and the standard enthalpy changes ($\Delta H°$) of −3.7 kcal/mol.

shows the plot of the amount of heat generated per injection as a function of the molar ratio of IACoA to the enzyme. The solid smooth line is the best fit of the data according to Wiseman et al. (*25*), yielding values for the stoichiometry of the MCAD−IACoA complex, association constant (K_a), and the standard enthalpy change ($\Delta H°$) of 0.65 ± 0.028, (2.6 ± 0.17) × 10^5 M^{-1}, and −3.67 ± 0.19 kcal/mol, respectively. Assuming a standard state of 1 M, the free energy of interaction ($\Delta G°$) of IACoA to MCAD can be calculated to be −7.4 kcal/mol. Given the magnitudes of $\Delta G°$ and $\Delta H°$, $T\Delta S°$ can be calculated to be 3.7 kcal/mol. An examination of these data suggests that unlike the binding of octenoyl-CoA to MCAD, which is enthalpically driven (*20*), the binding of IACoA to MCAD is dominated by both enthalpic and entropic contributions, albeit the entropic contribution decreases with an increase in temperature.

While investigating the temperature dependence of the MCAD + IACoA interaction, we realized that due to a smaller magnitude of $\Delta H°$ at lower temperatures, the above titration could not be reliably performed below 20 °C. Table 2 summarizes the temperature dependence of the thermodynamic parameters for the binding of IACoA to MCAD. From these data, it is apparent that as the temperature increases, $\Delta H°$ increases, and $T\Delta S°$ correspondingly decreases, resulting in a nearly invariant $\Delta G°$ value. Such a relationship has been referred to as the enthalpy−entropy compensation effect (*27*−*29*), and the origin of this effect has been attributed to a significant difference between $\Delta C_p°$

Table 2: Summary of the Thermodynamic Parameters for the Interaction of IACoA with MCAD[a]

T (K)	n	$10^{-5}K_a$ (M^{-1})	$\Delta H°$ (kcal/mol)	$\Delta G°$ (kcal/mol)	$T\Delta S°$ (kcal/mol)
293	0.72 ± 0.04	2.43 ± 0.21	−1.89 ± 0.13	−7.22 ± 0.05	5.33
298[b]	0.63 ± 0.06	2.37 ± 0.24	−3.52 ± 0.38	−7.33 ± 0.06	3.81
300.5	0.67 ± 0.02	2.94 ± 0.15	−3.76 ± 0.13	−7.52 ± 0.03	3.76
303[b]	0.57 ± 0.03	2.07 ± 0.15	−4.60 ± 0.34	−7.37 ± 0.04	2.77
305.5	0.60 ± 0.04	2.40 ± 0.22	−5.30 ± 0.43	−7.52 ± 0.06	2.22
308	0.77 ± 0.04	2.21 ± 0.17	−5.31 ± 0.31	−7.53 ± 0.05	2.22

[a] Determined via isothermal microcalorimetry. [b] Average of two experiments under identical conditions.

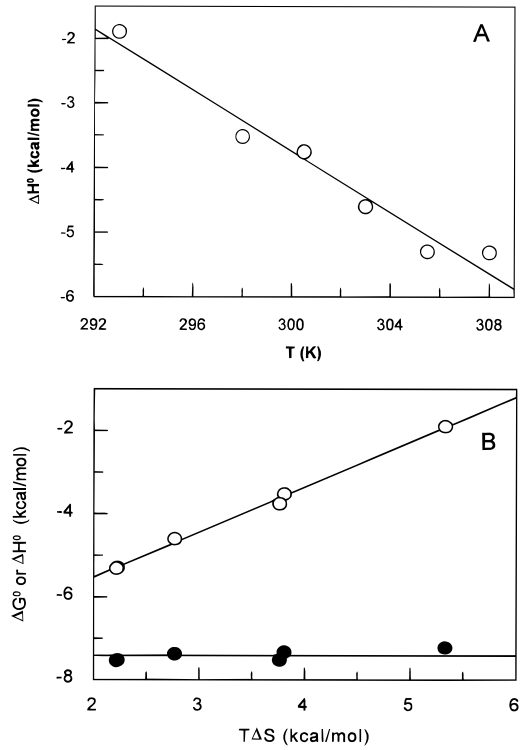

FIGURE 5: Effect of temperature on the thermodynamic parameters of the MCAD−IACoA complex. Panel A shows the temperature dependence of $\Delta H°$. The solid smooth line is the best fit of the data for a $\Delta C_p°$ (slope) of −0.237 (kcal/mol)/K. Panel B shows the enthalpy−entropy compensation plot. The dependences of $\Delta G°$ and $\Delta H°$ on $T\Delta S°$ are shown by solid and open circles, respectively. The linear regression analysis for the data of $\Delta H°$ versus $T\Delta S°$ yields the magnitudes of the slope and intercept of 1.08 and −7.698, respectively.

and $\Delta S°$ values (*30*). It should be pointed out that the stoichiometry of the MCAD−IACoA complex was found to fall in the range 0.57−0.77 via the microcalorimetry method. A qualitatively similar range (0.56−0.79) of the MCAD−IACoA complex was obtained from spectrophotometric titration of MCAD by IACoA (see Tables 1 and 2). These values are in contrast to the stoichiometry of the MCAD−octenoyl-CoA complex equal to 1 (*20*). We are currently investigating the origin of this discrepancy, and we will report these findings subsequently.

Figure 5 (top panel) shows the dependence of $\Delta H°$ on T. A linear regression analysis of these data yields the magnitude of $\Delta C_p°$ (slope) to be −0.24 (kcal/mol)/K. This value is somewhat less negative than that obtained for the binding of octenoyl-CoA to the enzyme (*20*). The bottom panel of Figure 5 shows the dependence of $\Delta G°$ (solid circles) and $\Delta H°$ (open circles) on $T\Delta S°$. The linear regression analysis of $\Delta H°$ versus $T\Delta S°$ data yields slope and intercept values of 1.08 and −7.70, respectively.

Transient Kinetics for the Binding and Dissociation of IACoA. To determine the magnitude of equilibrium constant for the isomerization step (see eq 2), i.e., the equilibrium constant between the MCAD−IACoA collision complex and the MCAD−IACoA isomerized complex, we employed the stopped-flow kinetic technique. The rate constant for the interaction of IACoA to the enzyme was determined by mixing these species ([MCAD] ≪ [IACoA]) via the stopped flow syringes. Figure 6 (top panel) shows the time courses for the increase in absorbance at 417 nm upon mixing MCAD and IACoA via the stopped-flow syringes at different temperatures. The solid smooth lines are the best fit of the data by a single exponential rate equation. As elaborated previously (*1*), the observed rate constants serve as a measure of $k_2 + k_{-2}$. From the data of Figure 6, it is evident that the rate constant increases with an increase in temperature. This is in marked contrast to a small (almost negligible) change in the association constant of the MCAD−IACoA complex, determined via both spectrophotometric and microcalorimetric methods (see above).

To extract meaningful information from the temperature dependence of the observed rate constants ($k_2 + k_{-2}$), we proceeded to determine the magnitude of k_{-2} by the acetoacetyl-CoA (being a competitive inhibitor of IACoA) displacement method. In this approach, a reaction mixture containing 2.5 μM MCAD and 18 μM IACoA was mixed with a saturating concentration of acetoacetyl-CoA (1 mM) via the stopped-flow syringes, and the time course for the decrease in absorption at 417 nm was monitored. During this experiment, the acetoacetyl-CoA-dependent displacement of IACoA from the MCAD−IACoA complex has been envisaged to proceed via the following sequence of steps (eq 6).

$$\text{MCAD}-\text{IACoA}^* \underset{k_2}{\overset{k_{-2}}{\rightleftharpoons}} \text{MCAD}-\text{IACoA} \rightleftharpoons \text{MCAD} + \text{IACoA} + \text{acetoacetyl-CoA} \rightarrow \text{MCAD}-\text{acetoacetyl-CoA} \quad (6)$$

As elaborated previously (*1, 21, 22*), in the presence of a saturating concentration of acetoacetyl-CoA, the time-dependent decrease in absorption at 417 nm, under the above experimental condition, conforms to a single-exponential rate law, and the observed rate constant is equal to k_{-2} of eqs 2 and 6.

Figure 6 (bottom panel) shows the reaction traces (decrease in absorbance at 417 nm) for the displacement of IACoA from the MCAD−IACoA complex by acetoacetyl-CoA as a function of temperature. The data are best fitted (solid smooth lines) by the single-exponential rate equation for the decrease in absorbance at 417 nm. Like the rate constant for interaction of IACoA to MCAD, the dissociation rate of IACoA from the MCAD−IACoA complex increases with an increase in temperature.

Having determined the magnitudes of $k_2 + k_{-2}$ and k_{-2} from the data of Figure 6, respectively, we calculated the magnitudes of k_2 ($k_2 + k_{-2}$ minus k_{-2}) as a function of temperature. On examination of k_2 and k_{-2}, it appears that

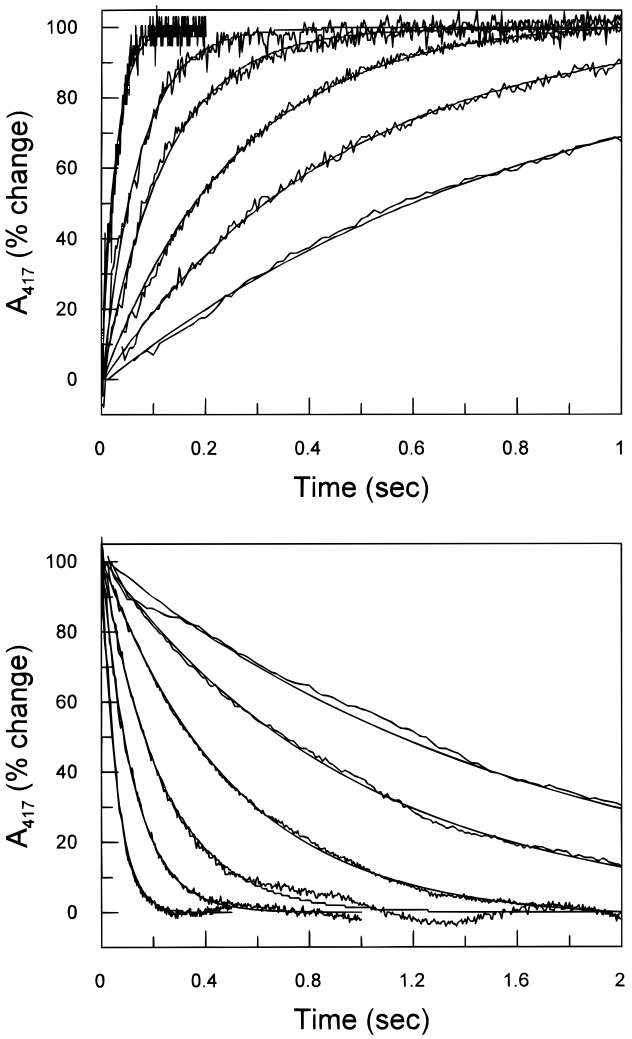

FIGURE 6: Effect of temperature on the transient rate constants for the interaction of IACoA with MCAD. Panel A (top) shows the time course for the increase in absorption at 417 nm upon mixing MCAD with IACoA ([MCAD] ≪ [IACoA]) via the stopped-flow syringes at different temperatures. The reaction traces from right to left are representative of the reaction temperature of 10, 15, 20, 24, 30, and 35 °C, respectively. The solid smooth lines are the best fit of the data for a single-exponential rate equation with observed rate constants of 1.2, 2.2, 3.8, 8.1, 14.2, and 36.8 s^{-1} at the above temperatures, respectively. Panel B (bottom) shows the time course for the displacement of IACoA from the MCAD−IACoA complex (measured at 417 nm) by a high concentration (1 mM) of acetoacetyl-CoA at different temperatures. The reaction traces from right to left represent the sequence of temperature as for the data of panel A. The solid smooth lines are the best fit of the data for a single-exponential rate equation, with observed rate constants of 0.62, 1.0, 2.0, 4.3, 8.2, 17.4 s^{-1} at the above temperatures, respectively. For clarity, the data of panels A and B are presented as the percent change of A_{417} as a function of time.

although these parameters individually increase as a function of temperature, their ratio is maintained at near unity at all temperatures. These results imply that the overall association constant for the binding of IACoA to MCAD is primarily contributed by the first step, i.e., equilibration between MCAD + IACoA and MCAD−IACoA collision complex.

Figure 7 shows the Arrhenius plots for the dependence of ln k_2 (open circles) and ln k_{-2} (open triangles) on 1/T. The solid lines are the linear regression analysis of both sets of the data according to eq 7, where A is the preexponential

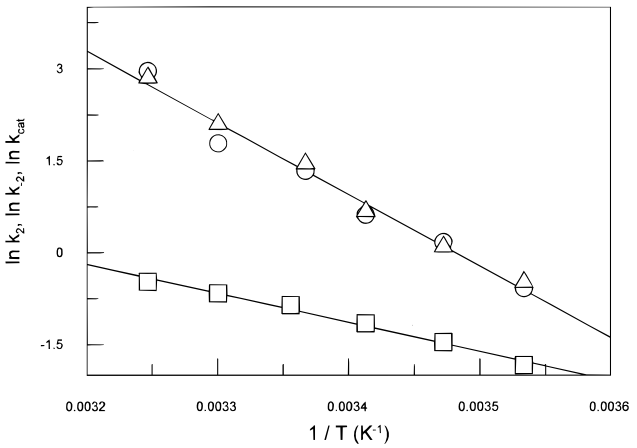

FIGURE 7: Arrhenius plots for k_2, k_{-2}, and k_{cat}. The temperature dependence of ln k_2, ln k_{-2}, and ln k_{cat} are shown by open circles, open triangles, and open squares, respectively. A common solid line represents the best fit of the data for the dependence of ln k_2 and ln k_{-2} on 1/T, with an energy of activation of 23.1 kcal/mol. The energy of activation obtained from the best fit of the ln k_{cat} versus 1/T data was 9.4 kcal/mol.

$$\ln k = \ln A - \frac{E_a}{RT} \tag{7}$$

factor, R is the universal gas constant, and E_a is the energy of activation. The magnitudes of ln A and E_a derived from these data were 40.7 and 23.1 kcal/mol, respectively.

From the above Arrhenius parameters, the difference in enthalpy ($\Delta H^{\ddagger}$) and entropy ($\Delta S^{\ddagger}$) between the ground and transition state of the isomerization reaction can be calculated by the following equations (eq 8). In eq 8B, k_B and h are

$$\Delta H^{\ddagger} = E_a - RT \tag{8A}$$

$$\Delta S^{\ddagger} = R \ln A - R \ln(k_B T/h) - R \tag{8B}$$

the Boltzmann constant and Planck's constant, respectively. Such calculations yield the magnitudes of $\Delta H^{\ddagger}$ (at 25 °C) and $\Delta S^{\ddagger}$ as 22.5 kcal/mol and 20.3 (cal/mol)/K, respectively.

We previously recognized an intrinsic similarity between the microscopic pathways for the binding of IACoA to MCAD and the IPCoA-dependent reductive half-reaction. Both these processes involve the formation of the enzyme−ligand collision complexes followed by slow isomerization reactions (*9*). We further elaborated that the k_{cat} for the IPCoA-dependent reaction is limited by the forward rate constant (equivalent to k_2 of eq 2) for the conversion of the MCAD−FAD−IPCoA Michaelis complex to the MCAD−$FADH_2$−IACoA charge-transfer complex (*7, 9*). In view of these facts, we investigated the temperature dependence of k_{cat} for the enzyme catalysis, by the steady-state kinetic method, utilizing saturating concentrations of IPCoA and $FcPF_6$. The Arrhenius plot of these data is also shown in Figure 7 (open squares). The solid line represents the best fit of the data according to eq 7. From these data, the magnitudes of E_a, $\Delta H^{\ddagger}$ (at 25° C), and $\Delta S^{\ddagger}$ were calculated (as described earlier) to be 9.4 kcal/mol, 8.8 kcal/mol, and −31 (cal/mol)/K, respectively.

DISCUSSION

By utilizing indoleacryloyl-CoA (IACoA) as a chromophoric reaction product for medium-chain acyl-CoA

dehydrogenase (MCAD), we could determine the magnitudes of the individual equilibrium constants for a two-step enzyme−ligand binding process (see eq 2) as a function of temperature. Given that the forward (k_2) and reverse (k_{-2}) rate constants for the second (isomerization) step are equal to unity at all temperatures, the overall observed binding constants (see Table 1) must be primarily contributed by the first step, i.e., the formation of the enzyme−ligand collision complex. Consistently, $\Delta G°$ for the second (isomerization) step would be equal to zero ($\Delta G° = -RT \ln K$), and thus the enthalpic ($\Delta H°$) and entropic ($T\Delta S°$) contributions (of the second step) would be balanced by each other. Under such a situation, if the enthalpic contribution is favorable, the entropic contribution would be unfavorable, and vice versa.

The question arises as to which of the above thermodynamic parameters is favorable during isomerization of the MCAD−IACoA collision complex. In attempting to answer this question, we performed model building studies for the interaction of IACoA with the MCAD site (data not shown) and observed that the carbonyl group of IACoA was hydrogen bonded (as observed with octenoyl-CoA; *18*) to both the 2′-ribityl hydroxyl group of FAD and the main chain amide nitrogen of Glu-376. Such hydrogen bondings have the potential to polarize the carbonyl group of IACoA, leading into an extended conjugation of the lone pair electron of the indole nitrogen to the carbonyl oxygen of the thiol ester (see eq 2). This results in a red-shift in the electronic spectrum of IACoA upon binding to the enzyme site (see eq 2). Since the red-shift in the IACoA spectrum occurs during the isomerization of the MCAD−IACoA collision complex, it is reasonable to assume that the above hydrogen bonds are formed exclusively during the isomerization step. The latter is likely to result in a favorable enthalpic and an unfavorable entropic contribution, so that the $\Delta G°$ value of the second (isomerization) step is maintained at zero. The above deduction is supported by the fact that the increase in temperature results in diminution of the 417 nm spectral band of the enzyme-IACoA complex (see Figure 2).

van't Hoff and Calorimetric Enthalpies for the Binding of IACoA to MCAD. It has been widely recognized that unlike calorimetric enthalpy (which is a direct measure of the amount of heat produced or consumed during macromolecule−ligand interactions), van't Hoff enthalpy is a derived parameter, whose magnitude is based on the variation in the binding constants as a function of temperature. For a two-step binding process, such as the interaction of IACoA with MCAD (eq 2), both steps are likely to produce or consume heat during the microcalorimetric titrations. In fact, since the second step involves the formation of a strong hydrogen bond (see above), it must contribute (at least in part) to the observed enthalpic changes discerned via microcalorimetry. On the other hand, since the equilibrium constant for the second step is maintained at unity at all temperatures, the van't Hoff enthalpy would be derived only from the first step (i.e., the formation of the MCAD−IACoA collision complex). We expected such a situation would cause a major discrepancy between the van't Hoff and calorimetric enthalpies, as observed in a number of cases (*26, 31*). However, in contrast to this expectation, we observed that the calorimetric enthalpy for the binding of IACoA to MCAD (−3.7 kcal/mol at 25 °C) is comparable to that derived from the linear and integrated van't Hoff plots (both yielding enthalpic changes in the range −3.4 to −3.8 kcal/mol). Such a similarity has been puzzling to us, and thus we are prompted to question the reliability of deduction of the van't Hoff enthalpy from small changes in the equilibrium constants as a function of temperature (see Table 1). Such a situation is likely to be encountered more frequently under conditions where there is a strong enthalpic−entropic compensation effect (yielding an invariant $\Delta G°$ value).

Temperature Dependence of the Thermodynamic Parameters for the Binding of IACoA to MCAD. As observed with a variety of protein−ligand complexes (*20, 32−34*), the calorimetric enthalpy for the binding of IACoA to MCAD exhibits a linear dependence on temperature (Figure 6), yielding a $\Delta Cp°$ value of −0.24 (kcal/mol)/K. This value is about 0.13 (kcal/mol)/K less negative than that observed for the binding of octenoyl-CoA to MCAD (*20*). At this point, it should be mentioned that both octenoyl-CoA and IACoA are constituted of hydrophilic and hydrophobic residues, which are expected to interact differently with water molecules in the solution phase. Likewise, prior to the binding of these ligands, the enzyme site cavity is likely to be filled/solvated by water molecules. Since no water molecules are retained at the interface of the MCAD−octenoyl-CoA complex (*18*), it follows that the binding of octenoyl-CoA/IACoA to the enzyme must involve desolvation of both CoA-ligand and the enzyme active site. Such desolvations are expected to contribute to the overall free energy of the enzyme−ligand complexes.

It has been frequently alluded to that a negative $\Delta Cp°$ value for the protein−ligand complex is primarily due to burial of nonpolar surface areas from the aqueous phase (*35−41*). Given that both IACoA and octenoyl-CoA molecules, as well as their complementary enzyme site phase, contain several nonpolar residues, and such residues are buried (desolvated) from the aqueous phase upon MCAD−IACoA/octenoyl-CoA interaction, their negative $\Delta Cp°$ values are not surprising. However, it is unclear as to why the $\Delta C_p°$ value obtained for the binding of octenoyl-CoA is more negative than that obtained with IACoA. Is this due to the difference in hydrophobicity between octenoyl-CoA and IACoA or is it due to the difference in specificity between octenoyl-CoA (a physiological reaction product of the enzyme) and IACoA for the enzyme site (*34, 42*)? The latter possibility is supported by the fact that the binding constant of octenoyl-CoA to the enzyme site is about 40-fold higher than that obtained for IACoA (*1, 10, 20, 22*).

From the data of Table 2 and Figure 5, it is evident that unlike $\Delta H°$, $\Delta G°$ for the binding of IACoA to MCAD is independent of temperature. Such a situation yields a strong enthalpy−entropy compensation effect, which has been observed with other protein−ligand complexes (*20, 27−29, 33, 43*). The origin of the enthalpy−entropy compensatory effect has been attributed to lie in the relative magnitudes of $\Delta S°$ and $\Delta C_p°$ (*30*). However, from the enthalpy−entropy compensation plot, it is evident that unlike the binding of octenoyl-CoA to MCAD (*20*), the binding of IACoA to MCAD involves a decrease in the magnitude of $\Delta H°$ (i.e., becoming less negative) with an increase in $T\Delta S°$. This is due to an increasing favorable entropic contribution to the

overall free energy at least in the temperature range between 20 and 35 °C.

From the entropy−enthalpy compensation plot (Figure 5, bottom panel), it can be calculated that when $T\Delta S°$ attains a zero value, $\Delta H°$ would be equal to −7.4 kcal/mol. The temperature at which $\Delta H°$ becomes equal to −7.4 kcal/mol can be calculated to be 43.5 °C (316.5 K) from the $\Delta H°$ vs T plot (Figure 5, top panel). Hence, at the latter temperature, the entropic contributions for the binding of IACoA to MCAD would be equal to zero. Since $\Delta S°$ is composed of both favorable and unfavorable entropic contributions, it follows that at 43.5 °C the former is balanced by the latter. The favorable entropic changes include solvent displacement (i.e., release of "frozen" water molecules in the bulk phase, often referred to as the hydrophobic effect; $\Delta S°_{HE}$) and an increase in vibrational modes (vibrational entropy; $\Delta S°_{v}$), whereas the unfavorable contributions include the loss in rotational−translational entropy ($\Delta S°_{rt}$) and conformational entropy ($\Delta S°_{conf}$). If the contribution of the vibrational entropy is considered negligible (*44*), $\Delta S°_{HE}$ is expected to be balanced by the sum of $\Delta S°_{rt}$ and $\Delta S°_{conf}$ at the above temperature. On the other hand, if $\Delta S°_{conf}$ is taken to be negligible, $\Delta S°_{HE}$ and $\Delta S°_{v}$ would be balanced by ΔS_{rt} (*42*). Hence, the calculation of the individual entropic changes at 43.5 °C would be dependent on the appropriateness of one of the above assumptions.

However, on the basis of all our data, suggesting that the binding of ligands to MCAD involves obligatory conformational changes (*1, 2, 7*−*10, 21, 22, 24*), the contribution of $\Delta S°_{conf}$ is unlikely to be negligible. Hence, we approximated the contributions of individual entropic changes according to Spolar and Record (*44*) and discerned the magnitudes of $\Delta S°_{HE}$, $\Delta S°_{rt}$, and $\Delta S°_{conf}$ to be +63.5, −50, and −13.5 cal/mol/K, respectively, at 43.5 °C.

Energetics of Polarization of the Carbonyl Group of IACoA. On the basis of the spectroscopic and transient kinetic data, we have proposed that the carbonyl group of IACoA is polarized within both the oxidized and reduced enzyme active sites, via an identical microscopic pathway (*1, 7*−*9*). The polarized form of IACoA also predominates upon conversion of the MCAD−FAD−IPCoA Michaelis/collision complex to the MCAD−$FADH_2$−IACoA charge-transfer complex during the reductive half-reaction of the enzyme (*7, 9*). As shown in eq 9, all these processes involve

$$\text{MCAD}-\text{FAD} + \text{IACoA} \rightleftharpoons \text{MCAD}-\text{FAD}-\text{IACoA} \rightleftharpoons \text{MCAD}-\text{FAD}-\text{IACoA}^* \quad (9A)$$

$$\text{MCAD}-\text{FADH}_2 + \text{IACoA} \rightleftharpoons \text{MCAD}-\text{FADH}_2-\text{IACoA} \rightleftharpoons \text{MCAD}-\text{FADH}_2-\text{IACoA}^* \quad (9B)$$

$$\text{MCAD}-\text{FAD} + \text{IPCoA} \rightleftharpoons \text{MCAD}-\text{FAD}-\text{IPCoA} \rightleftharpoons \text{MCAD}-\text{FADH}_2-\text{IACoA}^* \quad (9C)$$

the formation of an enzyme−ligand complex, followed by a subsequent isomerization step, which accompanies a red-shift in the IACoA spectral band. The only difference between these seemingly diverse reaction pathways is that the second (isomerization) steps of eqs 9A and 9B are devoid of "chemistry", whereas that of eq 9C is coupled to the oxidation/reduction process.

However, despite the above similarity, the energetics of polarization of the carbonyl-group of IACoA upon binding to MCAD-FAD and during the IPCoA-dependent reductive half-reaction are considerably different. For example, the enthalpic changes between the ground and transition states ($\Delta H^{‡}$) during the conversion of MCAD−FAD−IACoA to MCAD−FAD−IACoA* (eq 9A) is about 14 kcal/mol higher (i.e., unfavorable) than that obtained for the conversion of MCAD−FAD−IPCoA to MCAD−$FADH_2$−IACoA* (eq 9C). In contrast, the corresponding entropic changes ($\Delta S^{‡}$) during the former process is about 0.051 (kcal/mol)/K higher (i.e., favorable) than that of the latter. Hence, the transition state during the reductive half-reaction (eq 9C) is more stable enthalpically and less stable entropically than the corresponding transition state formed during the isomerization (coupled to the polarization of the carbonyl group) of the MCAD−FAD−IACoA collision complex (eq 9A). Relying on the fact that the ground state structures of the MCAD−FAD−IACoA and MCAD−FAD−IPCoA complexes are the same, the origins of the above energetic differences must lie in the transition state structures of the corresponding reactions. For example, on the basis that the attainment of the transition state is entropically favorable during the polarization of the carbonyl group of IACoA within the oxidized enzyme site, we propose that IACoA is more constrained in the ground state than in the transition state. The release of such a constraint (in the transition state) is likely to result in an increase in the activation entropy. A similar entropic gain is expected during the reductive half-reaction, but its magnitude would be offset by the loss of translation and rotational entropies of the reacting ligands (due to concertedness in proton and hydride transfers; *45*) within the transition state. We believe the latter is also responsible for a lower enthalpic difference between the ground and transition states during the reductive half-reaction vis à vis those obtained during the polarization of IACoA within the oxidized enzyme site. A further confirmation of these postulates must await structural investigations of the reduced enzyme−enoyl-CoA complex, as well as theoretical predictions of the relevant transition states.

ACKNOWLEDGMENT

We thank Kevin L. Peterson for his help in performing several experiments, critical review of the manuscript, and stimulating discussion.

REFERENCES

1. Johnson, J. K., Wang, Z. X., and Srivastava, D. K. (1992) *Biochemistry 31*, 10564−10575.
2. Johnson, J. K. (1994) Ph.D. Dissertation, North Dakota State University, Fargo, ND.
3. Beinert, H. (1963) *Enzymes 7*, 447−466.
4. Engel, P. C. (1990) in *Chemistry and Biochemistry of Flavoenzymes* (Muller, G., Ed.) Vol. 3, pp 597−655, CRC Press, Boca Raton, FL.
5. Thorpe, C. and Kim, J.-J. P. (1995) *FASEB J. 9*, 718−725.
6. Lehman, T. C., Hale, D. E., Bhala, A., and Thorpe, C. (1990) *Anal. Biochem. 186*, 280−284.
7. Johnson, J. K. and Srivastava, D. K. (1993) *Biochemistry 32*, 8004−8013.

8. Johnson, J. K., Kumar, N. R. and Srivastava, D. K. (1993) *Biochemistry 32*, 11575−11585.
9. Johnson, J. K., Kumar, N. R. and Srivastava, D. K. (1994) *Biochemistry 33*, 4738−4744.
10. Srivastava, D. K., Kumar, N. R. and Peterson, K. L. (1995) *Biochemistry 34*, 4625−4632.
11. Srivastava, D. K., Johnson, J. K., Kumar, N. R. and Peterson, K. L. (1996) in *Flavins and Flavoproteins* (Stevenson, K. J., Massey, V., and Williams, C. H., Jr., Eds.), pp 605−614, University of Calgary Press, Calgary.
12. Murfin, W. W. (1974) Ph.D. Dissertation, Washington University, St. Louis, MO.
13. Engst, S. and Ghisla, S. (1990) in *Flavins and Flavoproteins* (Curtis, B., Ronchi, S., and Zanetti, G., Eds.), pp 311−314, Walter de Gruyter, Berlin.
14. Lau, S., Brantely, R. K., and Thorpe, C. (1989) *Biochemistry 28*, 8255−8262.
15. Bernhard, S. A., Lau, S. J., and Noller, H. (1965) *Biochemistry 4*, 1108−1118.
16. Dunn, M. F., and Hutchinson, J. S. (1973) *Biochemistry 12*, 4882−4892.
17. Dunn, M. F., Biellmann, J., and Brandt, G. (1975) *Biochemistry 14*, 3176−3182.
18. Kim, J.-J. P., Wang, M., and Paschke, R. (1993) *Proc. Natl. Acad. Sci. U.S.A.* 90, 7523−7527.
19. Ghisla, S., Engst, S., Moll, M., Bross, P., Strauss, A. W., and Kim, J.-J. P. (1992) *New Developments in Fatty Acid Oxidation*, pp 127−142, Wiley-Liss, Inc.
20. Srivastava, D. K., Wang, S., and Peterson, K. L. (1997) *Biochemistry 36*, 6359−6366.
21. Kumar, N. R. and Srivastava, D. K. (1994) *Biochemistry 33*, 8833−8841.
22. Kumar, N. R. and Srivastava, D. K. (1995) *Biochemistry 34*, 9434−9443.
23. Thorpe, C., Matthews, R. G. and Williams, C. H., Jr. (1979) *Biochemistry 18*, 331−337.
24. Peterson, K. L., Sergienko, E. E., Wu, Y., Kumar, N. R., Strauss, A. W., Oleson, A. E., Muhonen, W. W., Shabb, J. B., and Srivastava, D. K. (1995) *Biochemistry 34*, 14942−14953.
25. Wiseman, T., Williston, S., Brandt, J. F., and Lin, L.-N. (1989) *Anal. Biochem. 17*, 131−137.
26. Liu, Y. and Sturtevant, J. M. (1995) *Protein Sci. 4*, 2559−2561.
27. Mukkur, T. K. S. (1978) *Biochem. J. 172*, 39−44.
28. Herron, J. N., Kranz, D. M., Jameson, D. M., and Voss, E. W., Jr. (1986) *Biochemistry 25*, 4602−4609.
29. Jin, L., Yang, J., and Carey, J. (1993) *Biochemistry 32*, 7302−7309.
30. Ha, J.-H., Spolar, R. S., and Record, M. T., Jr. (1989) *J. Mol. Biol. 209*, 801−816.
31. Naghibi, H., Tamura, A., and Sturtevant, J. M. (1995) *Proc. Natl. Acad. Sci. U.S.A. 92*, 5597.
32. Faergeman, N. J., Sigurskjold, B. W., Kragelund, B. B., Andersen, K. V., and Knudsen, J. (1996) *Biochemistry 35*, 14118−14126.
33. Jelesarov, I., and Bosshard, H. R. (1994) *Biochemistry 33*, 13321−13328.
34. Ladbury, J. E., Wright, J. G., Sturtevant, J. M., and Sigler, P. B. (1994) *J. Mol. Biol. 238*, 669−681.
35. Edsall, J. T. (1935) *J. Am. Chem. Soc. 57*, 1506−1507.
36. Privalov, P. L. (1979) *Adv. Protein Chem. 33*, 167−241.
37. Spolar, R. S., Ha, J.-H., and Record, M. T., Jr. (1989) *Proc. Natl. Acad. Sci. U.S.A. 86*, 8382−8385.
38. Livingstone, J. R., Spolar, R. S., and Record, M. T., Jr. (1991) *Biochemistry 30*, 4237−4244.
39. Makhatadze, G. I. and Privalov, P. L. (1990) *J. Mol. Biol. 213*, 375−384.
40. Makhatadze, G. I. and Privalov, P. L. (1993) *J. Mol. Biol. 232*, 639−659.
41. Murphy, K. P. and Gill, S. J. (1991) *J. Mol. Biol. 222*, 699−709.
42. Sturtevant, J. M. (1977) *Proc. Natl. Acad. Sci. U.S.A. 74*, 2236−2240.
43. Sigurskjold, B. W., Berland, C. R., and Svensson, B. (1994) *Biochemistry 33*, 10191−10199.
44. Spolar, R. S. and Record, M. T., Jr. (1994) *Science 263*, 777−784.
45. Pohl, B., Raichle, T., and Ghisla, S. (1986) *Eur. J. Biochem. 160*, 109−115.

BI9720585